

# Improving the Science Observing Efficiency of the Chandra X-ray Observatory via the Chandra Radiation Model

S. N. Virani<sup>a</sup>, J. M. DePasquale<sup>a</sup>, D. A. Schwartz<sup>a</sup>, R. A. Cameron<sup>a</sup>, P. P. Plucinsky<sup>a</sup>,  
S. L. O'Dell<sup>b</sup>, J. I. Minow<sup>c</sup> and W. C. Blackwell, Jr<sup>c</sup>

<sup>a</sup>Harvard-Smithsonian Center for Astrophysics, 60 Garden Street, Cambridge, MA, USA

<sup>b</sup>NASA Marshall Space Flight Center, Huntsville, AL, USA

<sup>c</sup>Jacobs Sverdrup, Marshall Space Flight Center, Huntsville, AL, USA

## ABSTRACT

The *Chandra* X-ray Observatory (CXO), NASA's latest "Great Observatory", was launched on July 23, 1999 and reached its final orbit on August 7, 1999. The CXO is in a highly elliptical orbit, with an apogee altitude of 120,000 km and a perigee altitude of 20,000 km, and has a period of approximately 63.5 hours ( $\approx 2.65$  days). It transits the Earth's Van Allen belts once per orbit during which no science observations can be performed due to the high radiation environment. The *Chandra* X-ray Observatory Center currently uses the National Space Science Data Center's "near Earth" AP-8/AE-8 radiation belt model to predict the start and end times of passage through the radiation belts. Our earlier analysis (Virani et al, 2000) demonstrated that our implementation of the AP-8/AE-8 model (a simple dipole model of the Earth's magnetic field) does not always give sufficiently accurate predictions of the start and end times of transit of the Van Allen belts. This led to a change in our operating procedure whereby we "padded" the start and end times of transit as determined by the AE-8 model by 10 ks so that ACIS, the Advanced CCD Imaging Spectrometer and the primary science instrument on-board *Chandra*, would not be exposed to the "fringes" of the Van Allen belts on ingress and egress for any given transit. This additional 20 ks per orbit during which *Chandra* is unable to perform science observations integrates to approximately 3 Ms of "lost" science time per year and therefore reduces the science observing efficiency of the Observatory. To address the need for a higher fidelity radiation model appropriate for the *Chandra* orbit, the *Chandra* Radiation Model (CRM) was developed. The CRM is an ion model for the outer magnetosphere and is based on data from the EPIC/ICS instrument on-board the Geotail satellite as well as data from the CEPPAD/IPS instrument on-board the Polar satellite. With the production and implementation of the CRM Version 2.3, we present the results of a study designed to investigate the science observing time that may be recovered by using the CRM for science mission planning purposes. In this paper, we present a scheme using the CRM such that for a modest increase in ACIS CTI, approximately 500 ks can be recovered each year for new science observations.

**Keywords:** *Chandra*, space missions, radiation environment, radiation belts, radiation models

## 1. INTRODUCTION

Very early in the mission, it was recognized that the National Space Science Data Center's "near Earth" AE-8/AP-8 radiation belt model was inadequate for science scheduling purposes.<sup>1</sup> In particular, our mission planning scheduling software uses only a simple dipole model of the Earth's magnetic field. The resulting B, L magnetic coordinates do not always give sufficiently accurate predictions of the start and end times of transit of the Van Allen radiation belts. This inadequacy of the AE-8/AP-8 model for the *Chandra* orbit was demonstrated by comparing the AE-8 model predictions for the entry and exit of radiation belt transit against the data from *Chandra*'s on-board radiation monitor, the *EPHIN* (Electron, Proton, Helium Instrument particle detector) instrument.<sup>3</sup> Since no other acceptable radiation model was available for use for scheduling purposes, and

---

Further author information: (Send correspondence to S.N.V.)

S.N.V.: E-mail: svirani@cfa.harvard.edu, Telephone: 1 617 496 7855

because of the radiation damage sustained very early in the mission by the front-illuminated (FI) CCDs of the ACIS instrument,<sup>4</sup> it was decided to simply “pad” the entry and exit times of the AE-8 model by 10 ks so that ACIS would not be exposed to the belt “fringes” while collecting science data, and therefore, to not exacerbate the radiation damage of the FI CCDs.

Since padding the AE-8 model predictions for radiation belt entry and exit, the *Chandra* X-ray Observatory had never triggered an autonomous safing procedure (known as “SCS 107”) because of poor radiation belt timing. Recently, a few triggers have occurred due to short transient events prior to predicted ingress into the outer electron zone. The Chandra Team is developing strategies for dealing with these electron spikes, which are not directly relevant to the discussion here. Nevertheless, the additional 20 ks per orbit for which ACIS must now be stowed to prevent further radiation damage translates into approximately 3 Ms of “lost” observing time per year. Therefore, with an improved radiation model, the 10 ks pad can perhaps be shortened and hence more time made available for science observations. In addition, a higher fidelity proton model that includes the asymmetric distribution of protons in the magnetosphere may predict the points in space and time along the *Chandra* orbit with significant fluxes of 100 keV to 200 keV protons which pose the most risk to the ACIS CCDs.

In order to better understand the *Chandra* radiation environment, as well as to better predict the entry and exit times for radiation belt transit, the *Chandra* Radiation Model (CRM) was developed by a group of scientists at Jacobs Sverdrup in consultation with scientists at Project Science/MSFC and the CXC/SAO.<sup>2</sup> CRMFLX, the database that “drives” the CRM, is an ion model for the outer magnetosphere. The model is based on data from the EPIC/ICS instrument on-board the *Geotail* satellite, as well as data from the CEPPAD/IPS instrument on-board the *Polar* satellite, and provides the user with flux values for 100 keV to 200 keV protons as a function of *Chandra* position and the geomagnetic activity index (“Kp” index). The CRM energy range was chosen because exposure to protons with energies of approximately 100 keV to 200 keV has been shown to produce an increase in the charge transfer inefficiency (CTI) and hence degraded energy resolution of the ACIS instrument.<sup>4</sup> Thus, the CRM was designed to be a tool for predicting encounters with magnetospheric regions rich in these particles.

With the CRM reaching a level maturity (current version is 2.3 – released May 2003), we initiated an in-depth study designed to explore the utility and merit of using the CRM for science scheduling purposes. In this paper, we present the results of this study. The outline of this paper is as follows. In Section 2 we outline our data selection methodology, while in Section 3 we present results and analysis. Conclusions follow in Section 4.

## 2. METHODOLOGY

In its highly eccentric orbit, *Chandra* experiences a complex radiation environment for the low-energy (here, 100–500-keV) protons. Outside the bow shock, the low-energy protons are solar protons quasi-embedded in the solar wind (with an intensity quite sensitive to solar activity — flares, coronal mass ejections, etc.). In the magnetosheath (between the bow shock and the magnetopause), the low-energy protons are shock-enhanced solar-wind protons plus leakage from the outer magnetosphere. In the outer magnetosphere, they are protons quasi-trapped in the earth’s magnetic field (with intensity sensitive to geomagnetic activity) plus solar protons partially penetrating the outer magnetosphere. In the inner magnetosphere, the trapped (radiation-belt) protons have very high intensities; hence, *Chandra* now always protects the science instruments against radiation damage while in this region. In addition to the *Chandra* position, the second input to the CRM database (the geomagnetic activity index, Kp) is also variable on a day to day basis. However, an analysis of Kp data from November 1963 to December 1999 (an interval which spans more than three complete solar cycles) determined that the most probable value is Kp=1.7 for the complete set of data, while the median is Kp=2.0, the mean is Kp=2.3, and the 95% level is Kp=5.0.<sup>2</sup> A separate analysis to determine the approximate flux-weighted average Kp —  $\langle Kp \rangle_{flux} = \ln_2 [2^{Kp}]$  — found a value of Kp=3.0 for the moving-average weighted Kp for a quarter-solar-cycle window. In the nominal case of *Chandra* operations, a weekly schedule of observations is finalized two weeks prior to the start of the observation, while the mission load is reviewed, finalized and approved approximately 1 week prior to load start. Thus, a reasonable estimate for the Kp must be made since the entry and exit times of radiation belt transit are required nearly 2 to 3 weeks prior to load execution. Given our Kp analyses, for this study we have adopted a fixed value of Kp=3.0.

The time periods of interest to this study are the 10 ks between the “Radiation Monitor disable” command and the time of the AE-8 predicted entry on ingress to perigee, and the 10 ks between the time of the AE-8 predicted exit from perigee and the time of the “Radiation Monitor enable” command. While the EPHIN detector operates throughout the orbit, the radiation-monitor process is disabled prior to perigee transit since the electron and proton rates rise dramatically during perigee transit and we do not wish the observatory to autonomously cease operations by triggering SCS 107. The density of damaging 100-200 keV protons in *Chandra*’s environs increases by approximately  $10^5$  in the radiation belts compared to the normal proton density during *Chandra*’s science operations at altitudes above  $\approx 70,000$  km. Thus, once science observations resume on egress from perigee, the radiation-monitor process is enabled to provide protection from high electron and proton rates that are associated with coronal mass ejections (CME) and large solar flares. Nevertheless, it is this 10 ks “pad time” on either side of perigee that we focus on since it is these intervals we wish to minimize via the CRM V2.3.

To simplify the problem, we decided to first study a 1-year period after solar maximum since the geomagnetic environment at that time is more representative of the environment that *Chandra* is likely to experience in the next 3-5 years rather than the environment it experienced after launch. This 1-year period is September 1, 2001 to September 1, 2002. Using a definitive *Chandra* ephemeris, a CRM V2.3 and an EPHIN database was produced that spans this time period.

While one year’s worth of EPHIN and CRM data were extracted to analyse, periods of time when *Chandra* was shut down due to an SCS 107 safing action because of high radiation rates due to a CME have been omitted from this study. When an SCS 107 radiation-induced shut down overlaps a perigee transit, the EPHIN data during those periods have been excluded from this analysis so as to compare only the “quiescent” EPHIN data against the CRM. While there are approximately 140 perigee transits per year, this data exclusion means that only 129 orbits were used on ingress and 126 orbits were used on egress for the September 1, 2001 to September 1, 2002 study.

### 3. RESULTS AND ANALYSIS

Figures 1 and 2 present scatter plots of CRM-predicted 100 keV to 200 keV proton fluxes against the lowest energy EPHIN proton channel (the “P4 channel”: protons with energies between 5 and 8.3 MeV) on ingress and egress, respectively. That is, the CRM and EPHIN P4 data between the time of the radiation monitor disable command and the time of the AE-8 predicted entry are plotted against one another in Figure 1, while the CRM and EPHIN P4 data between the time of the AE-8 predicted exit and the time of the radiation monitor enable command are plotted against one another in Figure 2. Since the EPHIN data are telemetered at 65-second intervals, whereas the CRM flux data are produced at 5 minute intervals, we have interpolated the EPHIN P4 data to correspond to the time vector for the CRM data. Data from September 1, 2001 to September 1, 2002 are plotted in “diamonds” while data from September 1, 2002 to June 1, 2003 are plotted using the “plus” symbols.

As is evident from the linear Pearson correlation coefficient, there is no correlation between the CRM V2.3 100 to 200 keV proton flux and the 5.0 to 8.3 MeV proton flux as measured by the EPHIN P4 proton channel. The absence of such a correlation is not surprising in that geomagnetic screening of 5-MeV protons is typically ineffective down to geosynchronous orbit. In lieu of a correlation between the CRM V2.3 100-200 keV proton flux and the EPHIN P4 channel flux, a method for determining the *greatest lower bound* on ingress and egress for the CRM V2.3 flux was developed. The *greatest lower bound* (hereafter *glb*) is the *maximum CRM flux such that an SCS 107 trip would not occur between the time of the radiation monitor disable command and the time of the AE-8 predicted entry on ingress, and between the time of the AE-8 predicted exit and the time of the radiation monitor enable command on egress*. By using this CRM *glb* flux on ingress and egress for mission planning purposes, we will demonstrate how a significant fraction of the “pad time” can be recovered for science observations.

The horizontal lines in Figures 1 and 2 denote the *glb* on ingress and egress for the two different time periods plotted. The value of the *glb* is determined as follows: it is the value of the largest CRM flux such that there would not be an SCS-107 safing event. On ingress, this has a value of  $2.0E4$  counts/sec/cm<sup>2</sup>/sr/MeV for the

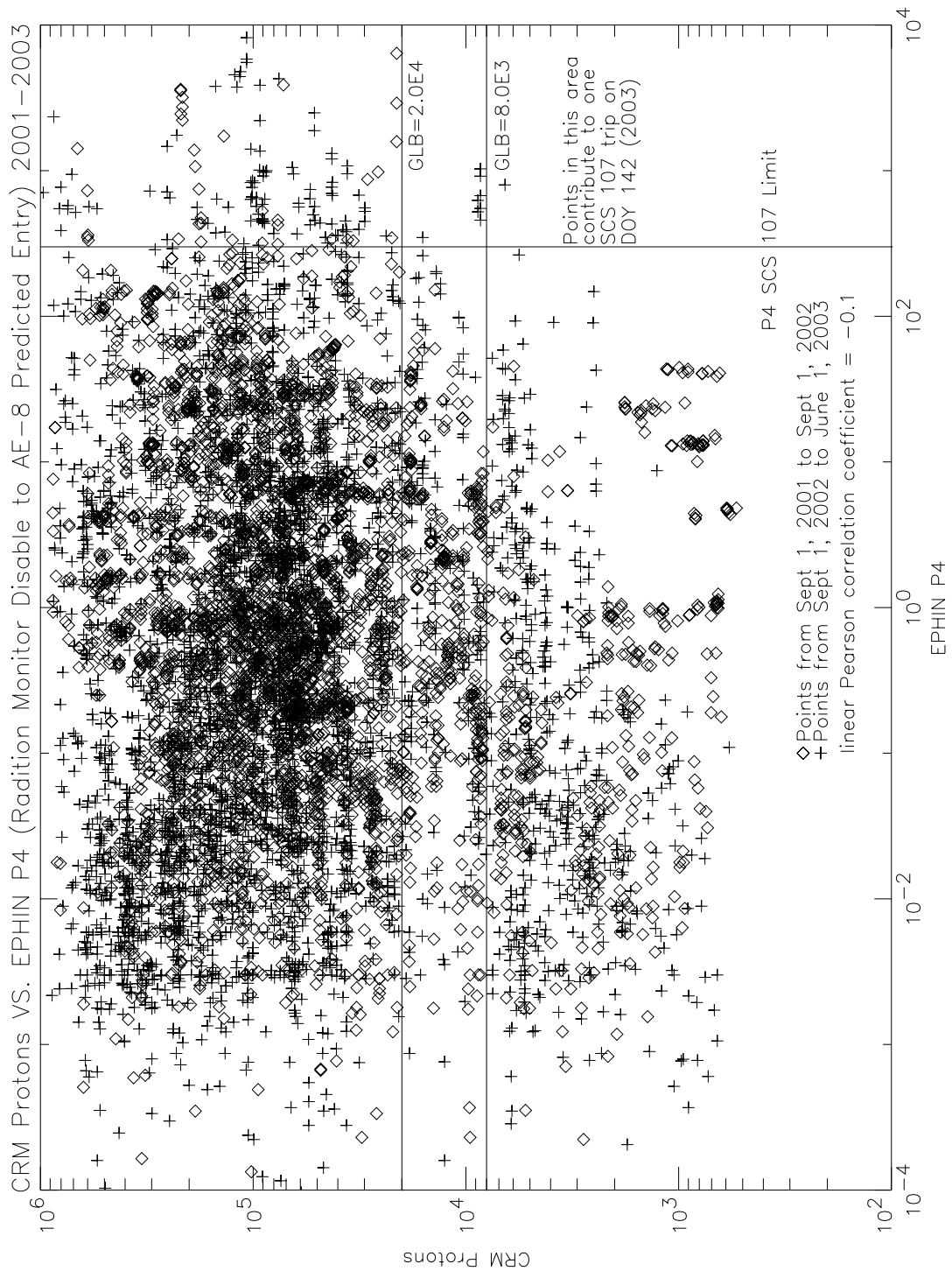


**Figure 1.** CRM protons versus EPHIN P4 scatter plot on ingress to perigee from September 1, 2001 to September 1, 2002 (diamond symbols) and from September 1, 2002 to June 1, 2003 (plus symbols).

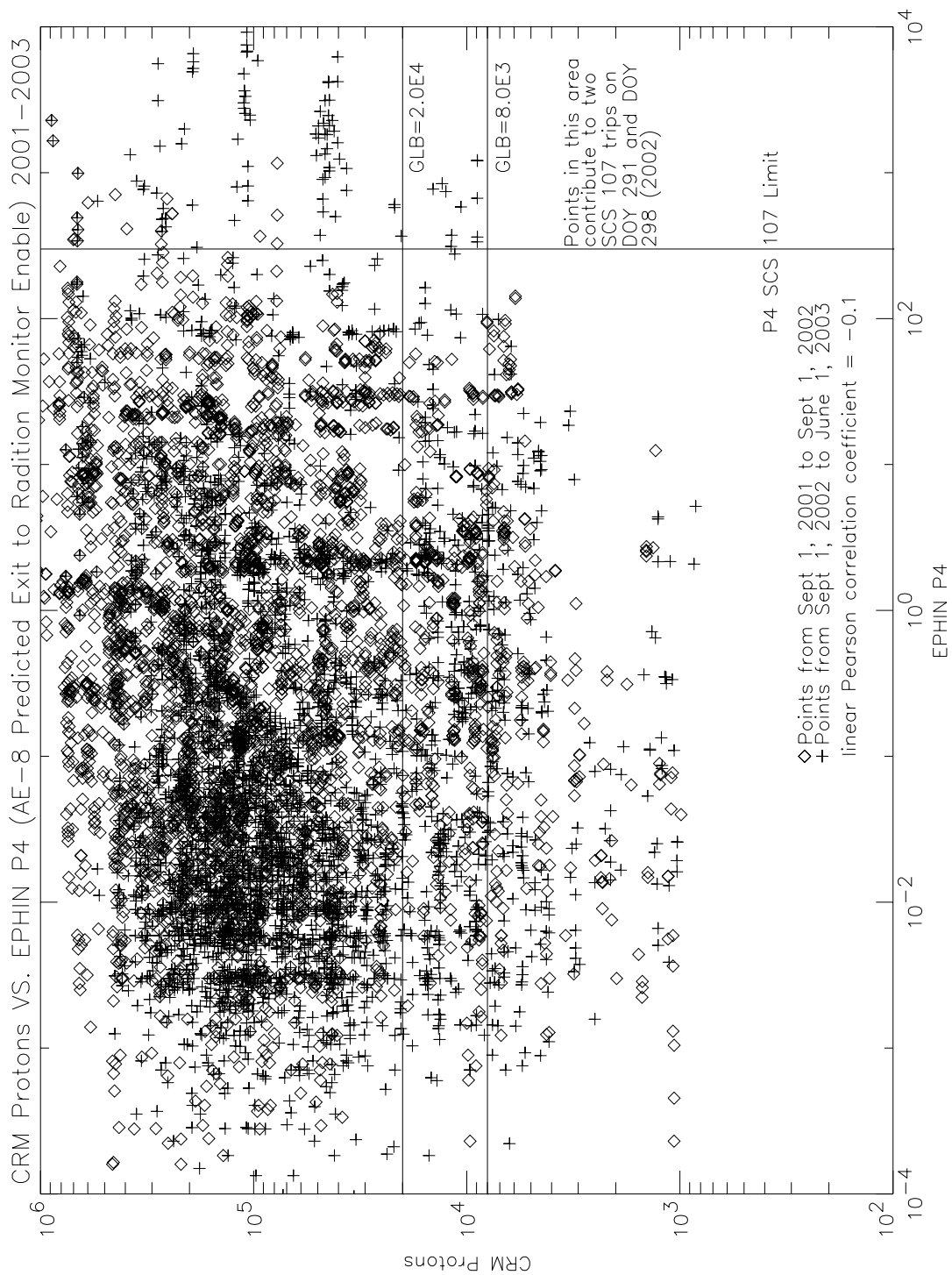


**Figure 2.** CRM protons versus EPHIN P4 scatter plot on egress from perigee from September 1, 2001 to September 1, 2002 (diamond symbols) and from September 1, 2002 to June 1, 2003 (plus symbols).

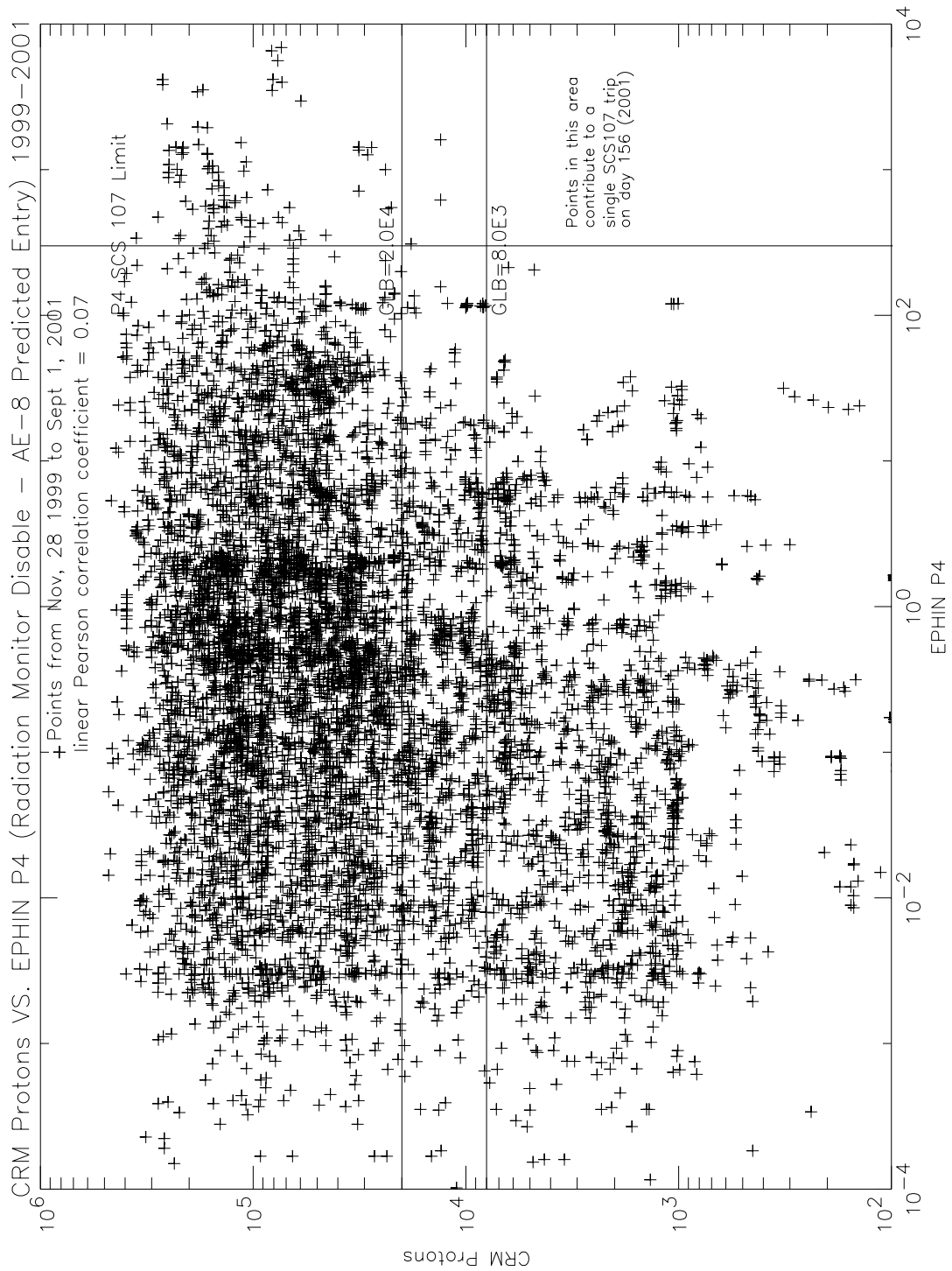


**Figure 3.** CRM protons versus EPHIN P4 scatter plot on ingress to perigee from November 28, 1999 to September 1, 2001.

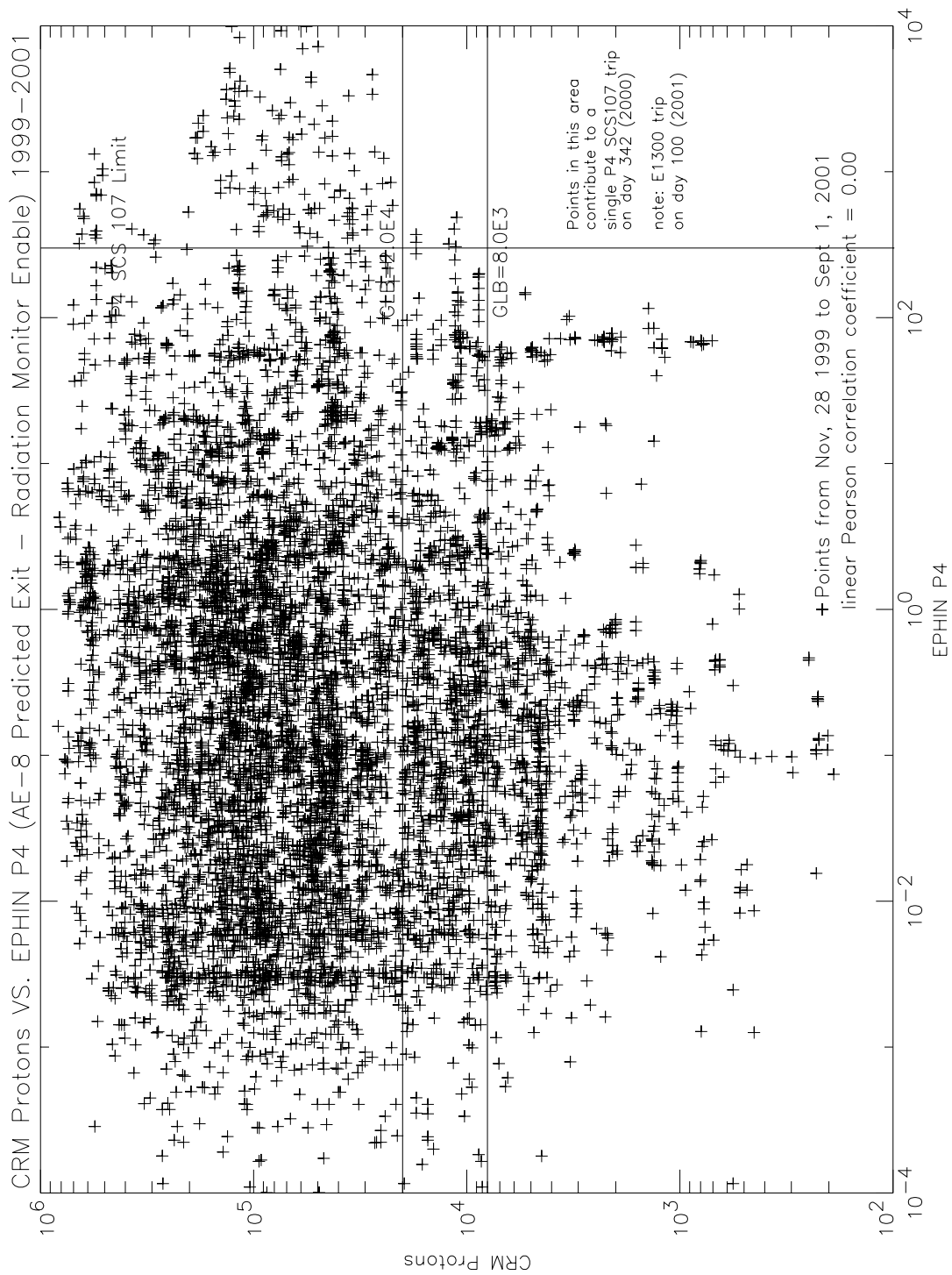


**Figure 4.** CRM protons versus EPHIN P4 scatter plot on egress from perigee from November 28, 1999 to September 1, 2001.

September 1, 2001 to September 1, 2002 time period. If this value was used for the September 1, 2002 to June 1, 2003 time period, there would be 1 SCS 107 trip as there are data points below 2E4 and to the right of the SCS 107 threshold for the EPHIN P4 channel. To avoid this 1 trip, the *glb* would have to be lowered to 8.0E3 — this is the second *glb* plotted on this figure. The *glb* value plotted on egress (Figure 2) for the September 1, 2001 to September 1, 2002 time period is the value determined on ingress for this same time period since the *glb* on egress can be increased by a nearly a factor of 2 (to 8E4 *counts/sec/cm<sup>2</sup>/sr/MeV*). (Please see our companion paper<sup>6</sup> in these proceedings for a discussion of possible seasonal variations). However, notice that using this *glb* on egress would have resulted in 2 SCS 107s trips during the September 1, 2002 to June 1, 2003 time period as there are data points below 2E4 and to the right of the SCS 107 threshold for the EPHIN P4 channel. It should be noted, however, that one data point in this region does not necessarily imply one SCS 107 safing sequence. In order for the radiation-monitoring process to activate SCS 107, there must be three consecutive readings above its threshold in at least one of the three channels it monitors. As on ingress, to avoid these 2 trips the *glb* would have to be lowered to 8.0E3 — this is the second *glb* plotted on this figure. As we stated previously, we wish to avoid SCS 107 trips as this results in the suspension of the science mission and requires ground intervention to resume science observations.

To determine how adequate these two *glbs* would have been in the first two years of the mission, similar scatter plots for ingress and egress were produced for the November 28, 1999 to September 1, 2001 time period. They are presented in Figures 3 and 4. As can be seen from Figure 3, using the larger *glb* of 2.0E4 *counts/sec/cm<sup>2</sup>/sr/MeV* on ingress would have resulted in 1 SCS 107 trip over this nearly two year period. This 1 SCS 107 trip would be avoided with the more conservative *glb* of 8.0E3 *counts/sec/cm<sup>2</sup>/sr/MeV*. On egress, the same result is found. Using a *glb* of 2.0E4 *counts/sec/cm<sup>2</sup>/sr/MeV* would have resulted in 2 SCS 107 trips — one induced by the EPHIN P4 channel and one by the EPHIN E1300 channel which counts electrons between 2.64 and 6.18 MeV. These three trips would be avoided with the lower *glb* of 8.0E3 *counts/sec/cm<sup>2</sup>/sr/MeV*.

**Table 1.** Recovered science time and additional CRM-calculated proton fluence on ACIS during *ingress* from November 28, 1999 to June 1, 2003 for *GLB* = 8.0E3 *counts/sec/cm<sup>2</sup>/sr/MeV*.

Time Interval	Recovered Science Time (ks)	Fixed-Kp CRM fluence	Observed-Kp CRM fluence	Additional CTI Increase	% of Pad Time Recovered
11/28/99 - 09/01/01	459.47	2.1E9	4.2E9	0.17%	19%
09/01/01 - 09/01/02	125.38	6.9E8	6.0E8	0.02%	10%
09/01/02 - 06/01/03	56.51	3.4E8	5.2E8	0.02%	6%
TOTAL	641.36	3.2E9	5.3E9	0.21%	AVG=12%

**Table 2.** Recovered science time and additional CRM-calculated proton fluence on ACIS during *ingress* from November 28, 1999 to June 1, 2003 for *GLB* = 2.0E4 *counts/sec/cm<sup>2</sup>/sr/MeV*.

Time Interval	Recovered Science Time (ks)	Fixed-Kp CRM fluence	Observed-Kp CRM fluence	Additional CTI Increase	% of Pad Time Recovered
11/28/99 - 09/01/01	695.83	5.1E9	7.3E9	0.29%	29%
09/01/01 - 09/01/02	226.26	2.0E9	1.6E9	0.05%	18%
09/01/02 - 06/01/03	82.78	6.8E8	2.5E9	0.07%	8%
TOTAL	1004.87	7.7E9	1.1E10	0.41%	AVG=21%



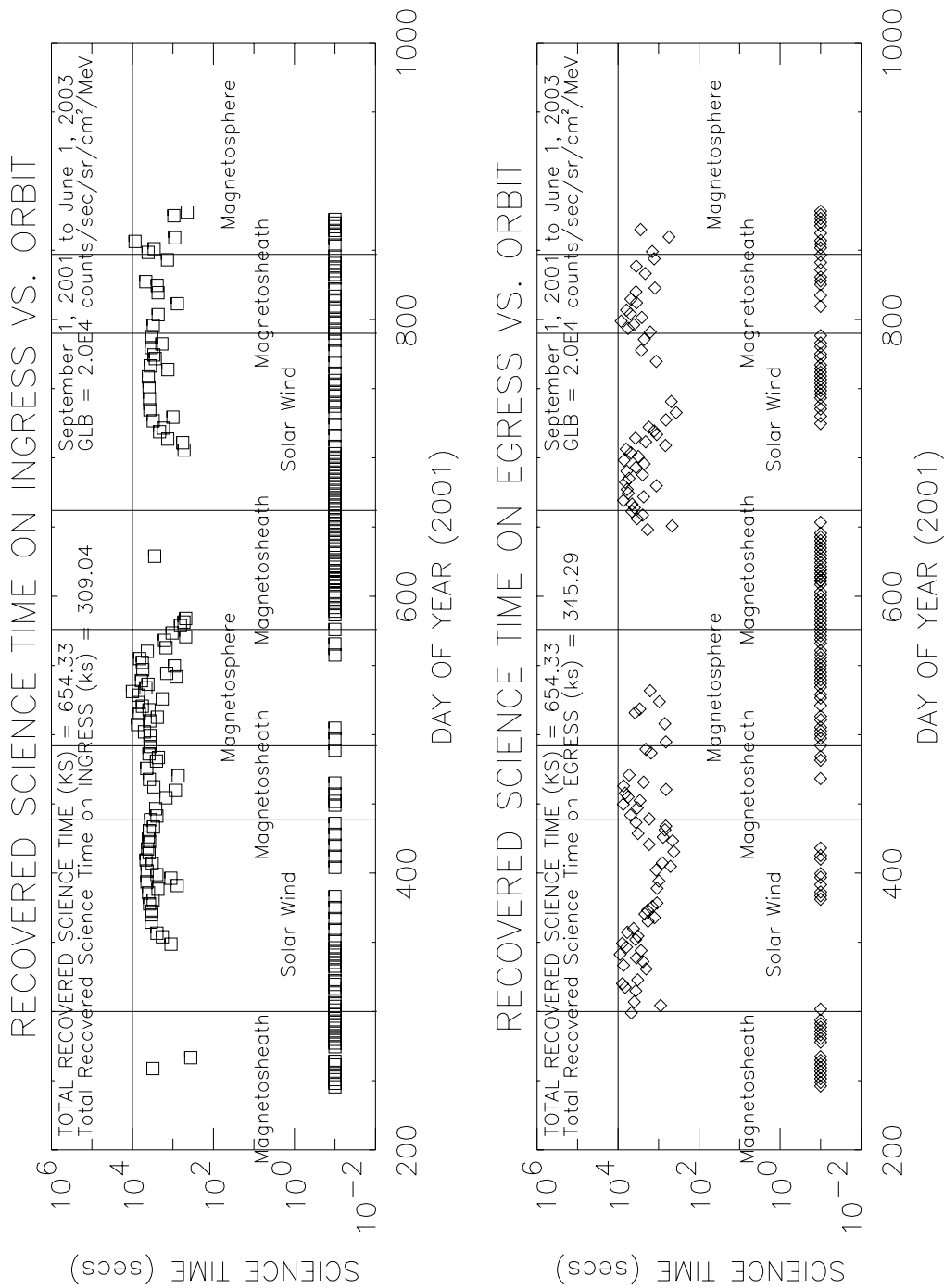
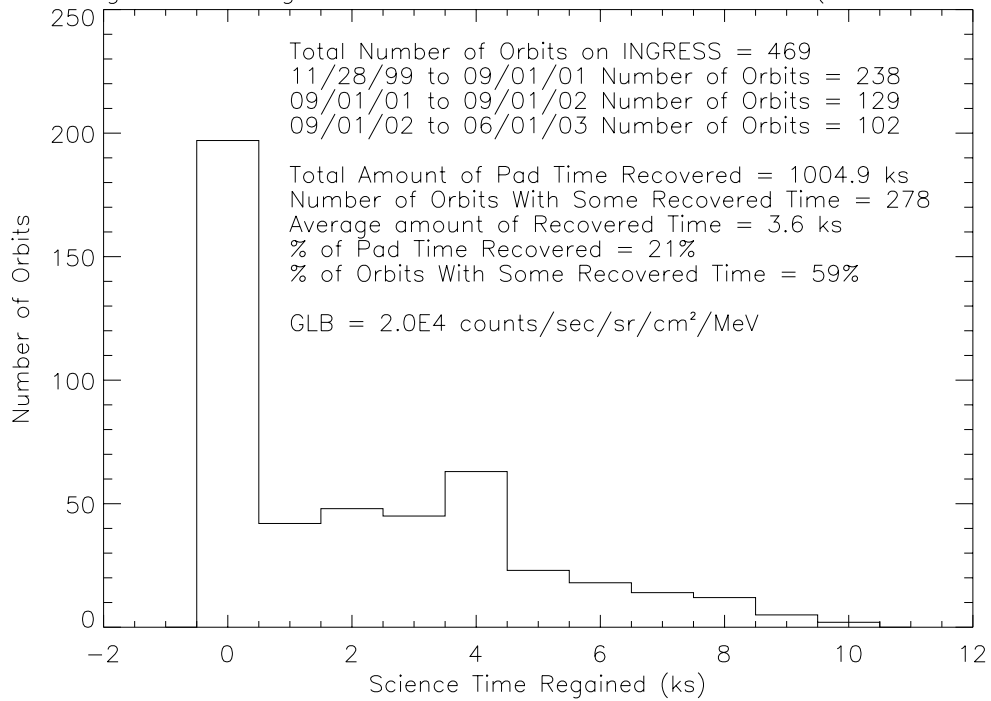


**Figure 5.** *Top Panel:* Recovered science time per orbit as a function of time on ingress for a *glb* of 2.0E4. Vertical lines indicate the location of Chandra’s apogee at that time of year. The horizontal line at 1e4 represents the current “pad time” and is therefore the maximum amount of time that can be recovered. Orbits with no science recovery time have been arbitrarily set to  $10^{-2}$ . *Bottom Panel:* Same as Top Panel – Recovered science time as a function of time on egress for a *glb* of 2.0E4. Notice that there appears to be some seasonal variation to the amounts of recovered science time. This observation is explored in-depth in our companion paper in this volume.<sup>6</sup>

Histogram of Regained Science Times on INGRESS (binsize=0.5ks)



Histogram of Regained Science Times on EGRESS (binsize=0.5ks)

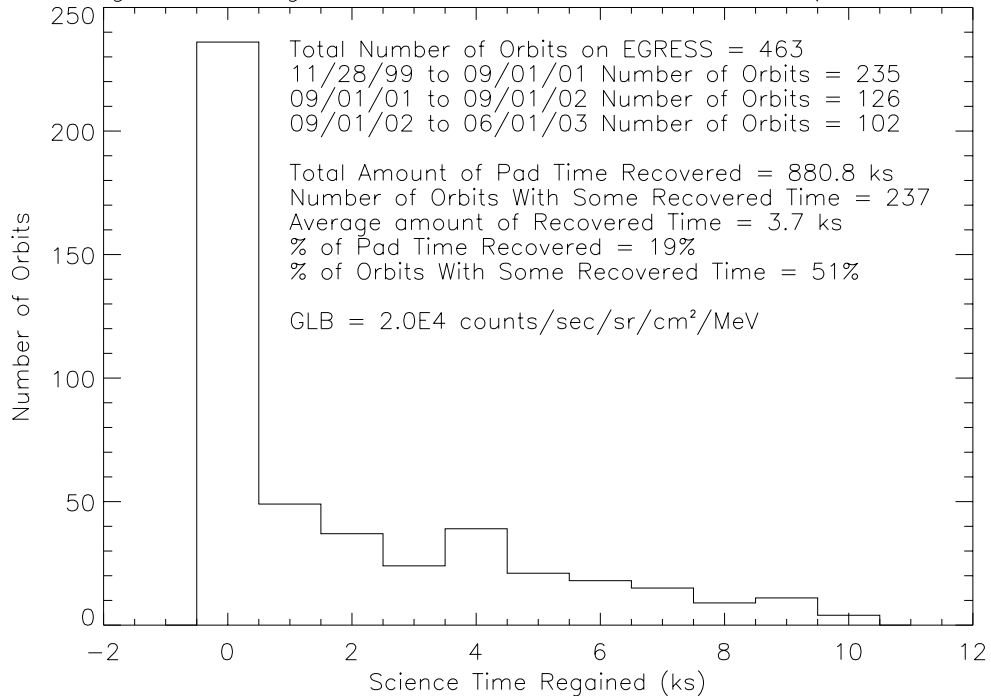


**Figure 6.** Histogram of orbits with science recovery time on ingress and on egress for a *glb* of 2.0E4. For nearly 55% of the orbits on ingress and egress between November 28, 1999 and June 1, 2003, an average of 3.7 ks of science time per orbit was recovered (see text).

Having determined two different *glb*s from the scatter plots presented in Figures 1-4, how can this be used to regain science time during the “pad time” on ingress and egress? The algorithm is relatively simple. On ingress, if the CRM flux is *greater* than the *glb* at the time of the radiation monitor disable command, no science time is recovered. Conversely, if the CRM flux is *less* than the *glb* at the time of the AE-8 predicted entry into the radiation zone, then the *entire* 10 ks has been recovered for science observations. However, as Figure 5 illustrates, very rarely is the entire “pad time” recovered on ingress. On average, the CRM flux exceeds the *glb* approximately 3.6 ks into the “pad time” for a *glb* of  $2.0E4 \text{ counts/sec/cm}^2/\text{sr/MeV}$  (see Figure 6). In fact, as Figure 6 demonstrates, for  $\approx 50\%$  of the orbits on ingress and egress no science time is recovered. The same algorithm can be applied on egress where the average amount of recovered science time for a *glb* of  $2.0E4 \text{ counts/sec/cm}^2/\text{sr/MeV}$  is approximately 3.7 ks.

**Table 3.** Recovered science time and additional CRM-calculated proton fluence on ACIS during *egress* from November 28, 1999 to June 1, 2003 for  $GLB = 8.0E3 \text{ counts/sec/cm}^2/\text{sr/MeV}$ .

Time Interval	Recovered Science Time (ks)	Fixed-Kp CRM fluence	Observed-Kp CRM fluence	Additional CTI Increase	% of Pad Time Recovered
11/28/99 - 09/01/01	459.47	2.1E9	1.1E9	0.04%	20%
09/01/01 - 09/01/02	61.09	3.2E8	2.4E8	0.01%	5%
09/01/02 - 06/01/03	55.26	3.3E8	2.3E8	0.01%	5%
TOTAL	575.82	2.8E9	1.7E9	0.06%	AVG=10%

**Table 4.** Recovered science time and additional CRM-calculated proton fluence on ACIS during *egress* from November 28, 1999 to June 1, 2003 for  $GLB = 2.0E4 \text{ counts/sec/cm}^2/\text{sr/MeV}$ .

Time Interval	Recovered Science Time (ks)	Fixed-Kp CRM fluence	Observed-Kp CRM fluence	Additional CTI Increase	% of Pad Time Recovered
11/28/99 - 09/01/01	535.50	4.8E9	6.1E9	0.24%	23%
09/01/01 - 09/01/02	177.26	1.8E9	1.2E9	0.04%	14%
09/01/02 - 06/01/03	168.03	1.7E9	1.1E9	0.03%	16%
TOTAL	880.79	8.2E9	8.4E9	0.31%	AVG=19%

As can be seen from Tables 1 to 4, a significant amount of science time can be recovered on both ingress and egress using this *glb* scheme for only a modest increase in ACIS CTI. In fact, nearly 2 Ms of science time would have been recovered on ingress and egress over the course of the mission to date using a *glb* of  $2.0E4 \text{ protons/cm}^2/\text{sr/MeV}$ . This translates into  $\approx 540$  ks of recovered science time per year. However, there would be 4 SCS 107 trips on egress that would subtract somewhat from the total regained science time. These SCS 107 trips could be avoided by using a lower *glb* of  $8.0E3 \text{ protons/cm}^2/\text{sr/MeV}$ . In this case, nearly 1.3 Ms of science observing time would have been regained over the course of the mission to date — approximately 350 ks per year. Alternatively, one could use the larger *glb* on ingress where only 2 SCS 107 trips were found but use the smaller *glb* on egress. Such a scheme would have yielded  $\approx 1.6$  Ms of recovered science time for an average yearly amount of 450 ks. However, these results also necessarily imply that ACIS would now be in the focal plane for a longer period of time. The consequence of this result means that ACIS would have additional exposure to low energy protons which has the potential to further damage the instrument. To quantify this additional proton exposure, we have computed the 100 to 200 keV proton fluence using the fixed Kp=3.0 CRM V2.3 database.

This is also tabulated in Tables 1 to 4. However, to estimate what the historical 100 to 200 keV proton fluence would be during these recovered science time periods, an additional CRM V2.3 database was generated using the World Data Center (WDC) *observed* Kp history since launch. One can therefore use this *observed*-Kp CRM V2.3 database to calculate what the historical ACIS exposure would have been during those recovered science time intervals on ingress and egress. Additionally, one can also calculate the total *observed*-Kp plus solar wind CRM V2.3 fluence during the 1 September 2001 to 1 September 2002 time period when ACIS was conducting science observations. We found this CRM fluence to be approximately  $1\text{E}11 \text{ protons}/\text{cm}^2/\text{sr}/\text{MeV}/\text{year}$ . Thus, by calculating what the additional ACIS CRM fluence would have been during each of these recovered science time intervals on ingress and egress, one can express this additional fluence as a percentage of the annual *observed*-Kp CRM fluence. Assuming that the change in ACIS CTI scales linearly with the change in CRM fluence,<sup>5</sup> one can therefore also estimate what the additional increase in ACIS CTI would be for a given *glb*. These numbers are also presented in Tables 1 to 4. Note that there are time intervals when the CRM fluence using the *observed*-Kp history is *less than* the CRM fluence using the fixed-Kp model. This indicates that during those time intervals, the Kp-weighted average flux corresponded to a Kp *less than 3.0*. Lastly, it should be noted that at present the CTI for the FI CCDs is growing at a rate of approximately 3% per year.

#### 4. CONCLUSIONS

In this paper, we have presented the results of a study designed to investigate the use of the CRM V2.3 in reducing the amount of “pad time” per orbit. In lieu of a correlation between the CRM and the EPHIN, we have developed a scheme known as the *greatest lower bound* that results in nearly 500 ks of recovered science time per year. Recognizing that regaining additional science time implies additional low energy proton exposure to ACIS, an attempt was made to calculate this exposure as well as to express it in terms of an additional CTI increase. This additional exposure is acceptable given the large amount of science time recovered. Thus, it is clear that for a modest increase in ACIS CTI, a significant fraction of the pad time can be recovered via the CRM for science observations. The ACIS instrument on-board the *Chandra X-ray Observatory* has returned some of the most exquisite, dramatic, and detailed images of the x-ray universe ever seen. The information returned, and the knowledge gained from these ACIS observations, has allowed us to explore another wavelength in rich detail that will undoubtedly propel astronomy forward in this new millenium. Gaining an additional 500 ks per year only accelerates this progress and increases our knowledge of the x-ray universe.

#### ACKNOWLEDGMENTS

We thank all of the engineers, technicians, and scientists who have made the *Chandra X-ray Observatory* such an outstanding success. The authors acknowledge support for this research from NASA contract NAS8-39073.

#### REFERENCES

1. S. N. Virani, R. Müller-Mellin, P. P. Plucinsky, and Y. M. Butt, “The Chandra X-ray Observatory’s Radiation Environment and the AP-8/AE-8 Model,” in *X-Ray Optics, Instruments, and Missions III*, J. Trümper and B. Aschenbach, eds., *Proc. SPIE*. **4012**, p. 669-680, 2000.
2. W. C. Blackwell, Jr, J. I. Minow, S. L. O’Dell, R. M. Suggs, D. A. Swartz, A. F. Tennant, S. N. Virani, and K. M. Warren, “Modeling the Chandra Space Environment,” in *X-Ray and Gamma-Ray Instrumentation for Astro. XI*, K. A. Flanagan and O. H. W. Siegmund, eds., *Proc. SPIE*. **4140**, p. 111-122, 2000.
3. R. Müller-Mellin, “EPHIN Response to the AXAF Radiation Environment”, *Doc. No. EPH-RRE-001*, Kiel, Germany, 1997.
4. G. Y. Prigozhin et al, “Radiation Damage in the Chandra X-ray CCDs”, in *X-Ray Optics, Instruments, and Missions III*, J. Trümper and B. Aschenbach, eds., *Proc. SPIE*. **4012**, p. 720-730, 2000.
5. R. A. Cameron et al, “Shelter from the Storm: Protecting the Chandra X-ray Observatory from Radiation”, in *Proc. ADASS XI* **281**, p. 132-135, 2002.
6. J. M. DePasquale et al, “A Study of the Seasonal Variations of the Chandra X-ray Observatory Radiation Model”, in *X-Ray and Gamma-Ray Instrumentation for Astronomy XIII*, K. A. Flanagan and O. H. W. Siegmund, eds., *Proc. SPIE*. **this volume**, 2003.